PERGAMON

Journal of Structural Geology 22 (2000) 589–602

JOURNAL OF STRUCTURAL GEOLOGY

www.elsevier.nl/locate/jstrugeo

The use of a combined structural, stable isotope and fluid inclusion study to constrain the kinematic history at the northern Variscan front zone (Bettrechies, northern France)

I. Kenis[a, b,*], Ph. Muchez[b], M. Sintubin[a], J.L. Mansy[c], F. Lacquement[c]

[a]*Laboratorium voor Algemene Geologie, KU Leuven, Redingenstraat 16, B-3000 Leuven, Belgium*
[b]*Fysico-Chemische Geologie, KU Leuven, Celestijnenlaan 200 C, B-3001 Leuven, Belgium*
[c]*Laboratoire de Sédimentologie et Géodynamique, USTL, URA CNRS 719, F-59655, Villeneuve d'Ascq cedex, France*

Received 7 April 1999; accepted 20 December 1999

Abstract

A detailed structural, stable isotope and fluid inclusion study of distinct vein generations has been performed in a kilometre-scale syncline to correlate the temperature–pressure conditions of vein formation with specific deformation episodes. The structural relationship of the veins with cleavage, folds, faults and with one another, allows the identification of pre-, syn- and post-Variscan carbonate vein generations. The stable isotope composition of the vein calcites and dolomites is very similar to that of the surrounding limestones and dolostones, respectively. This indicates that the cements were precipitated from fluids buffered by the host-rock and implies that the temperature–pressure characteristics of the fluids reflect the thermal history of the deformation history within the syncline. Microthermometric data of primary fluid inclusions were used to estimate the temperature–pressure conditions at precipitation time, and thus of the deformation. Pressure-corrected trapping temperatures for the veins show a temperature evolution from pre-Variscan ($\leq$310°C) to Variscan (260–200°C) and post-Variscan (75°C). This evolution indicates that the syncline developed not at a specific depth, but rather as an active, progressive deformation process during transport along the northern Variscan thrust front.

1. Introduction

Large-scale migration of fluids may be very important during orogenic deformation (Moore et al., 1990; O'Hara and Haak, 1992; Hodgkins and Stewart, 1994; Meere and Banks, 1997). During compression, faults and fractures play a key role in the fluid migration (Moore et al., 1988; Fischer and Byrne, 1990; Tobin et al., 1993). It is generally agreed that trace elements and isotopic signatures of vein cements may provide essential information on fluid sources, fluid flow, and exchange reactions between fluids and rocks (Burkhard and Kerrich, 1988). Pore-fluids are the medium in which carbon and oxygen are distributed between the rock (CO_3^{2-}) and fluid (HCO_3^-) reservoirs by dissolution and precipitation reactions (Meyers and Lohmann, 1985). The carbon and oxygen isotopic composition of the carbonate cements depends on the fluid–rock interaction and reflects the extent to which the diagenetic system is open or closed. If the fluid composition is completely controlled by exchange with the rock mass, precipitation takes place under rock-buffered conditions (Meyers and Lohmann, 1985; Gray et al., 1991). In an open system the fluid composition may show no relation to the rock.

The role fluids play in rock deformation opens a variety of possibilities for fluid inclusion research in solving tectonic problems. In this regard, Hodgkins and Stewart (1994) used fluid inclusions to constrain fault-zone pressure and temperature and the kinematic history in the Alpi Apuane (Italy). O'Hara and Haak (1992) examined fluid inclusions to obtain fluid

* Corresponding author.
E-mail address: ilse.kenis@geo.kuleuven.ac.be (I. Kenis).

0191-8141/00/$ - see front matter
PII: S0191-8141(99)00187-X

pressure and salinity variations in the footwall of the Rector Branch thrust (USA, North Carolina) and to evaluate the importance of fluid–rock interactions in the vicinity of faults and shear zones. Vrolijk (1987) developed a model for the fluid-migration history in convergent margins, based on fluid-inclusion analyses of syntectonic veins of the Kodiak accretionary complex (USA, Alaska). The thermal tectonic history of the subgreenschist facies Morcles nappe (Swiss Alps) has been unravelled by Kirschner et al. (1995) by applying oxygen isotope thermometry to quartz–calcite veins. The relative age of veins can be determined by using crosscutting and structural relationships between the veins and cleavage, bedding, folds and faults.

The primary aim of this study is the investigation of the fluid-flow system present during the deformation of Middle Devonian strata at the northern Variscan thrust front in northern France. Secondly, the temperature and pressure evolution during the deformation history at this thrust front, from burial and initial compression to uplift, has been constrained. Implications for the kinematic aspects of the Variscan orogeny will be discussed.

2. Geological setting

The frontal area of the Ardenne Allochthon (Fig. 1) is characterised by open, slightly north-verging, kilometre-scale folds. The allochthon is composed of Devonian and Carboniferous sedimentary sequences which rest unconformably on a Lower Palaeozoic basement. Deformation of this basement occurred before deposition of the Upper Palaeozoic strata. During the Variscan orogeny, the Ardenne Allochthon was folded and thrust along the Midi fault on the Brabant Parautochthon. Seismic reflection data show the Midi fault to be a detachment fault, slightly dipping (~5°) to the south (Fig. 2). The Givetian strata at Bettrechies are situated in the frontal area of the allochthon, ~10 km south of the surface trace of the Variscan thrust front (Midi fault; Figs. 1 and 2).

In the study area, there is an open, kilometre-scale syncline in a large quarry (Fig. 3). The Upper Givetian (Devonian) can be divided into four formations attaining a total thickness of more than 400 m in the stratotype region (Bultynck et al., 1991). This thickness decreases towards the north and at Bettrechies it is thought not to exceed 250 m (Boulvain et al., 1994). In the quarry, only the two upper formations, Mont d'Haurs and Fromelennes, are exposed. The Mont d'Haurs Formation is characterised by argillaceous, dark limestones and is followed by the dark limestones of the Fromelennes Formation. The limestones are affected by dolomitisation. The whole sequence is generally composed of thick-bedded carbonates alternating with thin argillaceous intercalations, which played an important mechanical role during the Variscan deformation (Mansy et al., 1995).

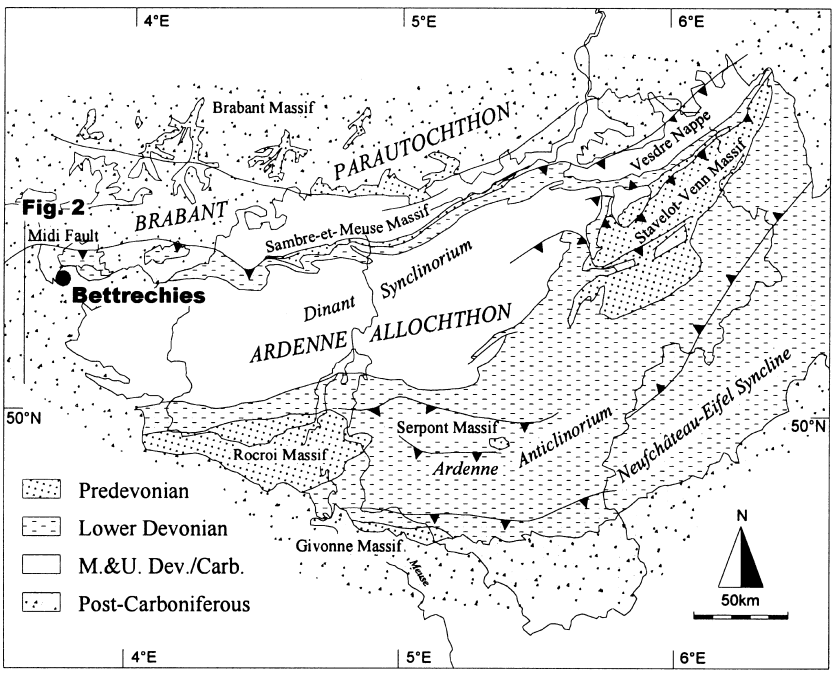

Fig. 1. Location of the study area in the frontal zone of the Ardenne Allochthon.

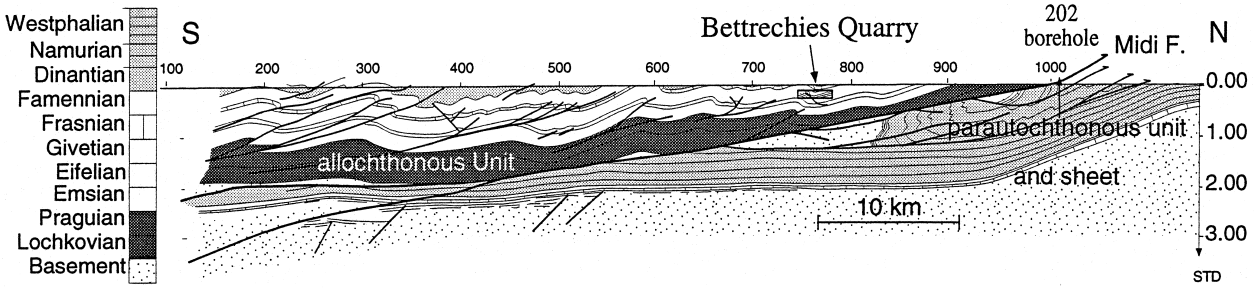

Fig. 2. Geological section between Mons and Valenciennes (after Mansy et al., 1997).

3. Structural framework

In the Bettrechies quarry, there is an asymmetric kilometre-scale syncline with a south-dipping axial surface (Fig. 3). The syncline is bounded by two anticlines with different morphologies, the southern anticline being open and the northern one being kink-shaped (Mansy et al., 1995). The northern limb of the syncline has an average dip of 40° towards the south, while the southern limb shows an average dip of 75° towards the north (Lacquement, 1996).

At metric- and decametric-scales, fault-bend folds can be observed on both limbs of the syncline. On the southern limb the decametric fault-bend fold (P_1) occurs associated with the fault ramp (R_1). The smaller, second fault-bend fold (P_1') is located on the back of P_1. The fault ramp R_1 is crosscut by the major thrust fault (F) which caused a displacement of ~15 m. The depth of this southern fault is unknown. On the northern limb of the syncline, the fault-bend fold (P_2) is associated with the second fault ramp (R_2) (Fig. 3). This fault R_2 is crosscut by the northern thrust-fault F', which joins the southern thrust-fault F at the lower level of the quarry. A sedimentological study indicates that the faults F and F' pass at the same stratigraphic level on both limbs (Mansy et al., 1995). They are located at the contact between the Mont d'Haurs and Fromelennes Formations, which is characterised by many argillaceous intercalations. The sense of displacement of the faults F and F' is opposite.

In addition to the structures that formed during progressive folding, a large set of strike-slip faults is present. At the lowest level of the quarry, the strike-slip fault V can be recognised (Fig. 3). The depth of V is unknown. This fault V is characterised by ankerite cementation and crosscuts the fault F.

Within the entire syncline a penetrative cleavage has been observed, whose development is closely related to the folding (Khatir, 1990; Mansy et al., 1995). The Variscan orogeny was responsible for the major part of the deformation (Mansy et al., 1995). During folding and faulting many fractures, now filled with cement, were formed. Mansy et al. (1995) used structural observations to obtain a relative chronology of the continuous and progressive deformation. In this chronology the cleavage is taken as reference. During progressive folding, the accommodation of the syncline was accomplished mostly by bedding-slip and fault-bend folding. In the first stage, the fault-bend folds P_1, P_1' and P_2 were formed. All three of them are crosscut by the cleavage. At a later stage, progressive folding resulted in additional slipping and/or thrusting. The faults F and F' post-date the cleavage and former fault ramps R_1 and R_2.

4. Methodology

The geometric features and paragenetic sequence of the veins were described in the field. Particular attention was paid to the relationship between the veins on the one hand and the cleavage, faults and folds on the

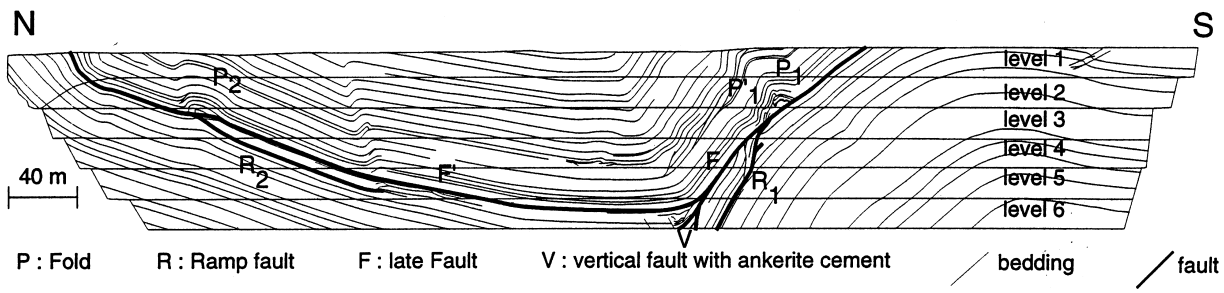

Fig. 3. North–south section of the synclinal structure in the quarry of Bettrechies.

other. Forty stained samples and ~60 thin sections of the veins and host-rock were examined by conventional and cathodoluminescence microscopy to refine the paragenetic sequence. Dolomite phases were identified by staining with alizarine red and iron-rich carbonate phases by staining with potassium ferricyanide (Dickson, 1966). Cathodoluminescence microscopy was carried out with a Technosyn Cold Cathodo-Luminescence Model 8200 MK II at 16–20 kV, 620 μA gun current, 0.05 Torr vacuum and 5 mm beam width. Three milligram samples of the veins and host-rock were drilled from polished surfaces to determine their carbon and oxygen isotopic composition on a Finnigan–Mat Delta-E mass spectrometer. The aliquots were reacted with 2 ml of 100% orthophosphoric acid under vacuum at 25°C. The mass spectrometric analyses were corrected according to Craig (1957), using repeated analysis of NBS-19 (TS-limestone). Isotope data are expressed as per mil (‰) deviation from the Vienna Pee Dee Belemnite (VPDB) standard. Reproducibilities determined from replicate analyses of split samples were better than 0.1‰ for oxygen and better than 0.05‰ for carbon at the 2σ level. Four samples were selected for a microthermometric analysis. The fluid inclusions were examined on a Linkam heating–cooling stage. A detailed description of the sample preparation technique and the measurement procedure has been given by Muchez et al. (1994). The final melting temperature of ice (T_m ice) was reproducible to within 0.2°C and the homogenisation temperature (T_h) to within 3°C. Observations were made on fluid inclusions occurring in growth zones and therefore interpreted as being primary in origin (Goldstein and Reynolds, 1994). Re-equilibration of fluid inclusions to lower densities, inducing higher homogenisation temperatures, may occur during intracrystalline deformation of crystals. Thermometric measurements were made in the vicinity of the less strained zones (if present) of the crystals. Strongly deformed zones (e.g. intensely twinned zones in calcite) were avoided to minimise the analysis of stretched or leaked fluid inclusions.

5. Geometry and petrography of the vein generations

During folding and faulting numerous fractures were formed. Based on crosscutting relationships of the veins with other structural features, on the petrographic data and on the chronological scheme of the deformational structures present in the quarry (Mansy et al., 1995), five major groups of veins can be distinguished. Each group can be associated with a deformation episode in the development of the syncline. The first group consists of veins with a pre-Variscan deformation origin. The veins of the second, third and fourth group all formed during the Variscan deformation. A metric duplex structure, which formed in response to the Variscan folding, is found in the quarry. In this duplex structure, pure dolomite veins occur associated with completely dolomitised limestones. Moreover, pure dolomite veins have been recognised only in dolostones indicating a mineralogical control of the host-rock on the vein composition. This would imply that the necessary ions are derived from the surrounding dolostones and that ambient fluid was at least partly in chemical equilibrium with the host rock. Due to a lack of crosscutting relations with other structural features, it is impossible to classify the dolomite veins into the second, third or fourth major group. The fifth group consists of veins that formed after the Variscan deformation.

5.1. Group I: pre-Variscan deformation

This group represents veins with an orientation perpendicular to the bedding (Fig. 4a). They are displaced along the bedding plane during bedding slip. The cleavage is penetrative and crosscuts the veins. The veins are composed of two calcite phases, a non-ferroan phase followed by a ferroan one. The non-ferroan calcite phase shows a homogeneous orange luminescence, while the ferroan phase shows sector zonation. The crystals of both phases are characterised by an undulatory extinction and show an intense development of twin planes that are sometimes bent (Fig. 4b). The development of the curved twins can be related to intracrystalline deformation (e.g. Burkhard, 1993). The calcite cements are stylolitised and the orientation of the stylolites is parallel to the vein walls (Fig. 4c). The veins probably formed during the burial stage: the progressive burial of the sediments during deposition caused a bedding normal compression inducing the formation of fractures perpendicular to the bedding.

5.2. Group II: Variscan deformation, pre-cleavage

The second group can be divided into two subgroups. A first subgroup represents veins, which occur along the fault plane R_2 and in a brecciated zone below and connected to this fault plane. Their calcite veins show an intense development of twin planes (Types II and III of Burkhard, 1993). Their occurrence probably indicates an origin of the veins related to the activity of the fault R_2. This fault is associated with the ramp fold P_2, which is considered by Mansy et al. (1995) to predate cleavage development.

The second subgroup of veins is present along the fault plane R_1 and parallel to the bedding (Fig. 4d). The veins are characterised by a ferroan calcite composition and are also crosscut by stylolites. Calcite twin planes are intensely developed (Types III and IV of

Burkhard, 1993) and crystals show undulatory extinction. The veins along the fault plane show shear discontinuities and wall-rock inclusions indicating a syn-fault R_1 origin (Ramsay and Huber, 1983). This fault was responsible for the formation of the ramp fold P_1, which predates cleavage development. The group II veins, parallel to the bedding, crosscut the group I veins, perpendicular to the bedding (Fig. 4a). Shear discontinuities and wall-rock inclusions are present, in this case indicating a syn-bedding-slip origin (Ramsay and Huber, 1983). An intersection-lineation of the cleavage and the veins is seen as small cracks (Fig. 5a). Therefore the veins are interpreted to predate cleavage development.

5.3. Group III: Variscan deformation, syn-cleavage

Sigmoidal, en-échelon, ferroan calcite veins are oriented oblique to the bedding and perpendicular to the cleavage (Fig. 5b). The general orientation of the veins and the cleavage with respect to the bedding plane indicates an out-of-syncline shear movement on the bedding plane (top-to-the-south on the southern limb, top-to-the-north on the northern limb). The group III veins are crosscut by the cleavage, but in general, they are not dissolved along the cleavage planes. Sigmoidal veins, which are not crosscut by the cleavage, are also present. The calcite shows a bright orange luminescence and several quartz crystals occur dispersed in the calcite cement. In some places the quartz crystals are broken. They show a sweeping undulatory extinction while the calcite crystals show an intense development of twin planes (Types III and IV of Burkhard, 1993), both referring to an intracrystalline deformation. No traces of dynamic recrystallisation, which would be shown by the formation of new subgrains, have been observed in the quartz crystals. In thin sections, the cleavage penetrates the vein walls at certain places (Fig. 5c). This indicates a pre-cleavage origin. In other zones, the cleavage orientation is controlled by the veins, indicating a post-cleavage origin

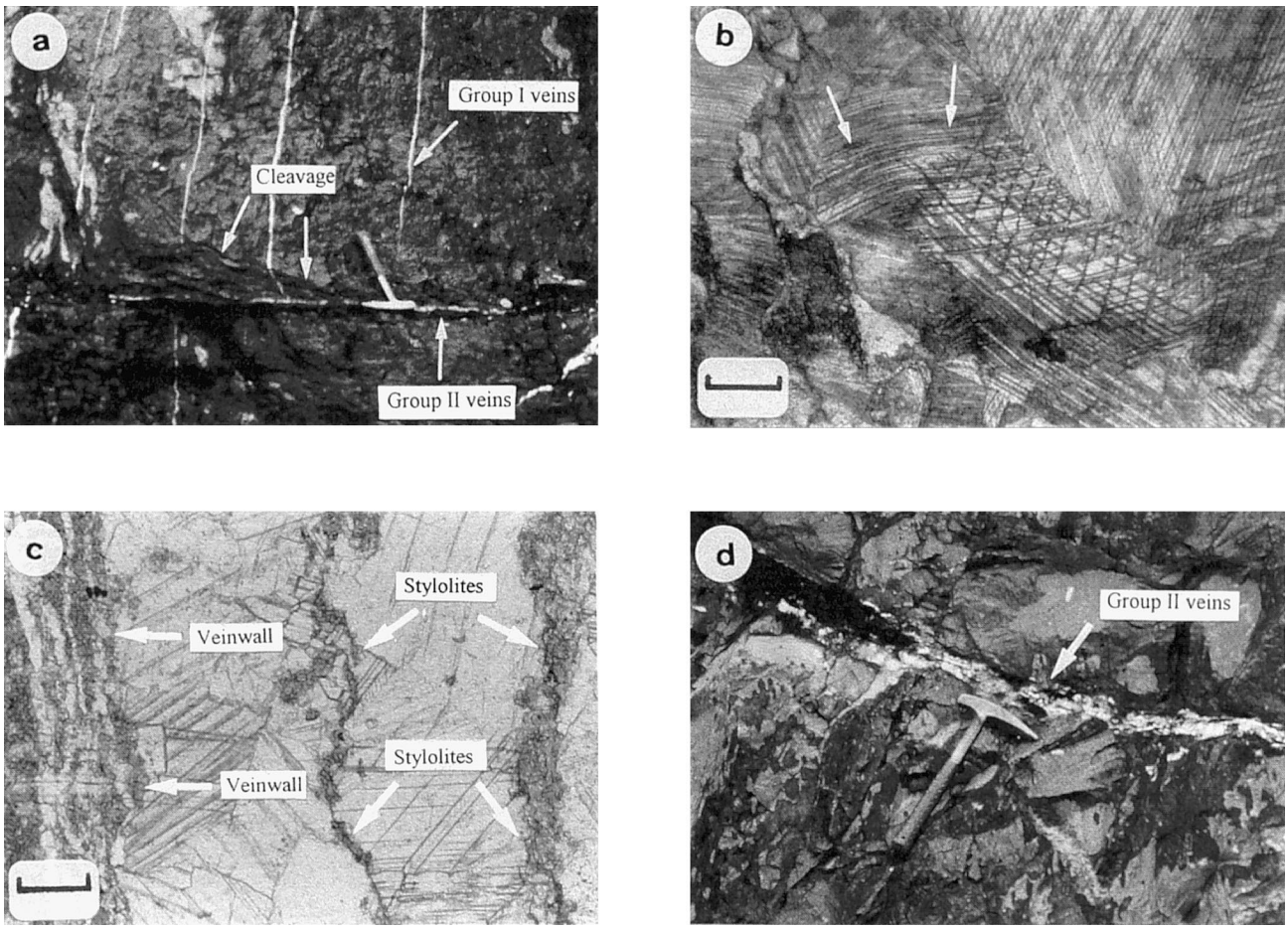

Fig. 4. The different vein groups. (a) Geometry of the pre-Variscan calcite vein group I (hammer is 33 cm). (b) Occurrence of curved twins, related to intracrystalline deformation (group I, plane-polarised light, scale bar is 0.32 mm). (c) Pre-Variscan veins of group I, crosscut by numerous stylolites parallel to the vein walls (plane-polarised light, scale bar is 0.32 mm). (d) A first generation of calcite veins which are oriented parallel to the stratification. They are classified within the Variscan, pre-cleavage group II veins (hammer is 33 cm).

(Fig. 5d). Therefore a syn-cleavage origin is opted for. Within the veins, vein parallel stylolites are present.

5.4. Group IV: Variscan deformation, post-cleavage

The veins of the fourth group can be subdivided into three subgroups. A first subgroup represents veins that occur along the fault plane F' and along a small backthrust, related to the fault F'. The veins are composed of ferroan calcites with a uniform dull to bright orange luminescence. The vein cements are stylolitised and shear-discontinuities indicate a syn-fault F' origin. Twin planes may be strongly developed (Types III and IV of Burkhard, 1993). Undulatory extinction is present. The veins are not crosscut by the cleavage. The latter is in accordance with the chronological model of Mansy et al. (1995) where fault F' is classified as being post-cleavage.

A second subgroup represents a second generation of veins present along the bedding plane. No wall-rock inclusions are observed. The calcites are composed of blocky calcite crystals, showing a homogeneous dull to bright luminescence. Stylolitisation is well developed. Typical calcites have an undulatory extinction and show an intense development of twin planes, which are sometimes bent. The veins crosscut the cleavage, indicating a post-cleavage origin.

A third subgroup is characterised by en-échelon veins which are formed by an antithetic shear couple (R' shears) that is oriented roughly 70° to the shear couple of fault F. This probably indicates a syn-fault F origin. The veins are composed of a non-ferroan dolomite generation (red zoned luminescence) and a light-ferroan calcite generation (homogeneous yellow luminescence). Calcite twin planes are weakly developed and undulatory extinction is rare. The veins are not crosscut by the cleavage.

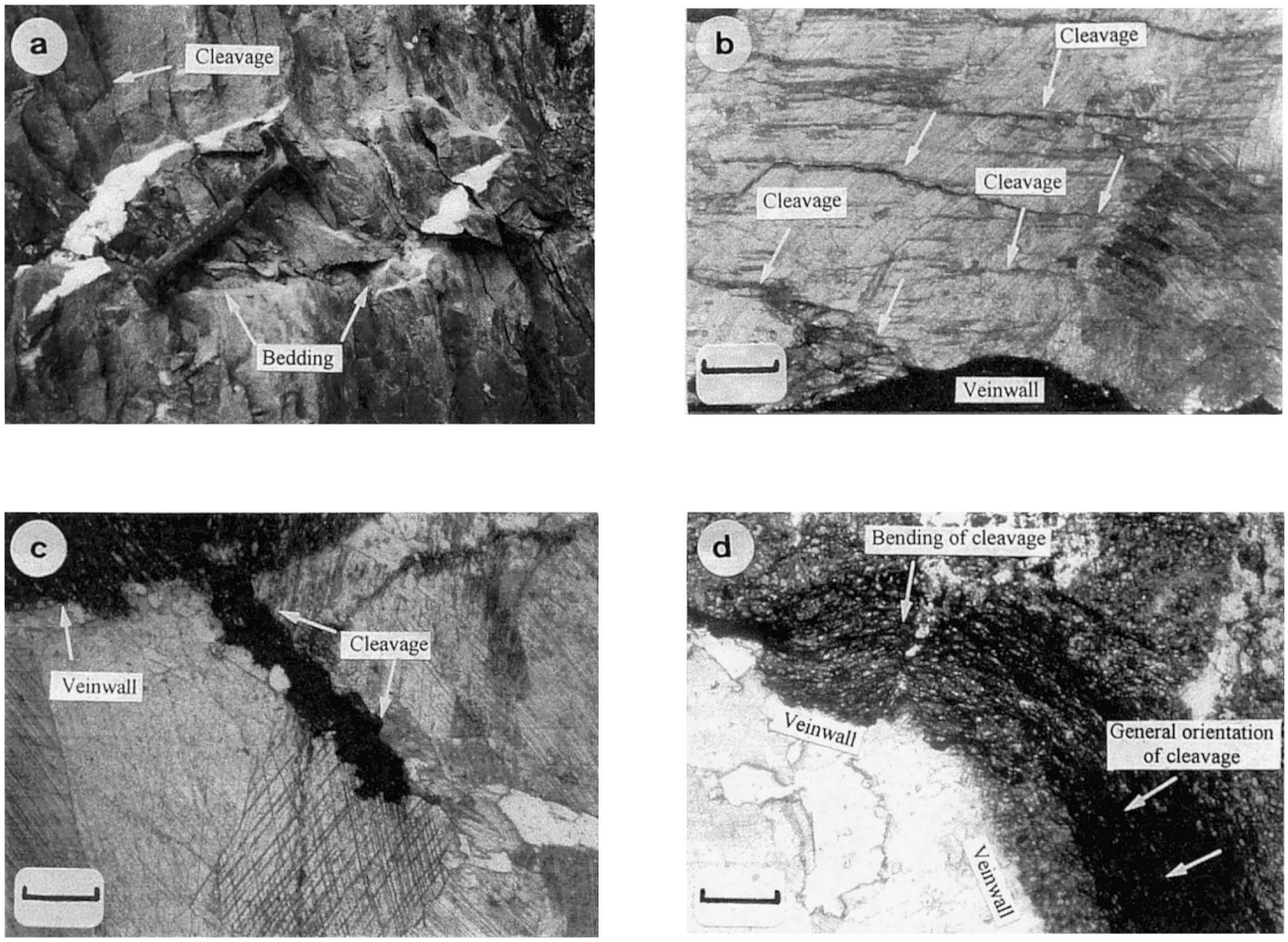

Fig. 5. The different vein groups. (a) Cleavage (arrows) clearly crosscuts the Variscan group II veins (plane-polarised light, scale bar is 0.27 mm). (b) Variscan syn-cleavage veins (group II), oriented oblique to the bedding (hammer is 33 cm). (c) Cleavage (arrow) penetrates the Variscan group II veins (plane-polarised light, scale bar is 0.32 mm). (d) Cleavage bends around the Variscan group III veins (plane-polarised light, scale bar is 0.32 mm).

5.5. Group V: post-Variscan deformation

The last group represents veins that occur along strike-slip faults crosscutting the Variscan fold and faults and therefore are interpreted as formed after the Variscan folding and faulting. This group can be subdivided into multiple generations. Carbonate cements have been taken along the fault plane V (Fig. 6). Two veins have been investigated: a non-ferroan granular calcite vein showing a well-developed sector zonation under cathodoluminescence and a fibrous ankerite vein with a zoned luminescence. The crystals of both vein types show only weakly developed twin planes. The second vein type is unique within the quarry because of the ankerite cement. The post-Variscan veins, which occur along other strike-slip faults, have not been investigated.

5.6. Overview

In the Bettrechies synclines many fractures were formed during deformation. Structural and petrographic examination allows the recognition of five major vein groups fitting in the chronology of the quarry. Veins perpendicular to the bedding were classified within the first group and are probably formed during the burial stage due to bedding normal compression. The second group represents veins that are Variscan pre-cleavage in origin. The veins are crosscut by the cleavage or related to the movement of the fault ramps R_1 and R_2. The latter implies that they were formed synchronous with the faults R_1 and R_2 and thus with the associated ramp folds P_1 and P_2. Since these folds are crosscut by the cleavage, they are pre-cleavage in origin as are the faults and related veins. The sigmoidal en-échelon veins are classified within the third group and are probably syn-cleavage in origin. They were formed due to a bedding-slip movement accomplishing the accommodation of the syncline during progressive folding. The fourth group represents veins, which were formed during the Variscan orogeny and postdate cleavage development. They crosscut the cleavage or are related to the movement of the faults F and F'. These faults have been defined as post-cleavage in the chronological model of Mansy et al. (1995). The last group of veins is present along the fault planes of strike-slip faults that crosscut the syncline and are formed after the Variscan deformation.

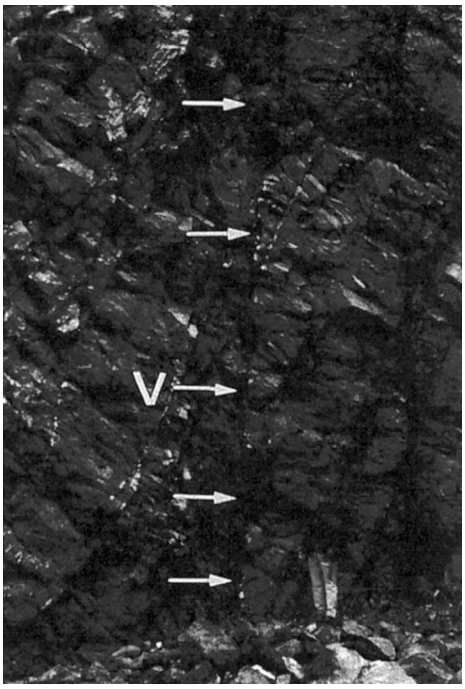

Fig. 6. The transverse fault V at the lower level of the quarry at Bettrechies. Person is 1.75 m.

6. Stable isotope analysis

6.1. Pre-Variscan vein cements

The oxygen and carbon isotopic composition of the pre-Variscan veins varies between −6.1‰ and −5.9‰ VPDB and between −0.79‰ and −0.46‰ VPDB, respectively (Fig. 7; Table 1). These values fall within the range of the stable isotopic composition of the surrounding limestones ($\delta^{18}O = -7.9‰$ to −5.4‰ VPDB; $\delta^{13}C = -1.15‰$ to 1.18‰ VPDB) (Fig. 7; Table 1).

The similarity of the stable isotopic composition of the veins and of the surrounding limestones could be due to precipitation of the calcite cements from a fluid in which isotopic composition was buffered by the surrounding rock (Gray et al., 1991; Marquer and Burkhard, 1992; Muchez et al., 1995). Rock-buffering

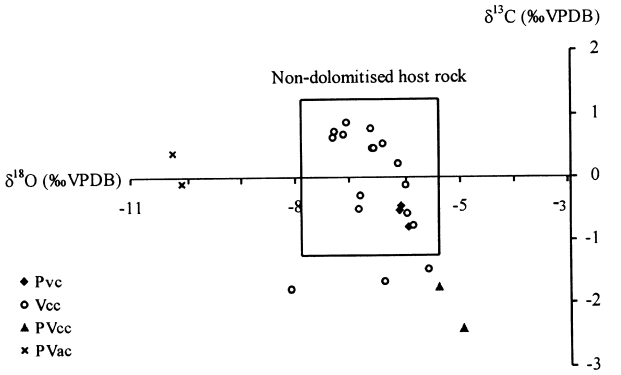

Fig. 7. Carbon and oxygen isotopic composition of the Givetian limestones (n = 20) and of the pre-Variscan (Pvc), Variscan (Vcc), post-Variscan calcite (PVcc) and ankerite (Pvac) vein cements (n = 25).

Table 1
Stable isotope data of the Bettrechies vein cements and host-rock. *Dhr* — dolomitised host-rock, *pVc* — pre-Variscan cements, *Vcc* — Variscan calcite cements, *Vdc* — Variscan dolomite cements, *PVcc* — post-Variscan calcite cements, *PVac* — post-Variscan ankerite cements

Sample	$\delta^{13}C$ (‰ VPDB)	$\delta^{18}O$ (‰ VPDB)	Sample	$\delta^{13}C$ (‰ VPDB)	$\delta^{18}O$ (‰ VPDB)
Dhr1	−0.6	−3.9	*Vcc1*	0.86	−7.1
Dhr2	−0.67	−3.8	*Vcc2*	0.73	−7.3
Dhr3	−0.78	−3.8	*Vcc3*	0.68	−7.1
Dhr4	−0.6	−3.8	*Vcc4*	0.45	−6.6
Lhr1	−1.07	−7.5	*Vcc5*	0.23	−6.1
Lhr2	1.18	−6.5	*Vcc6*	0.54	−6.4
Lhr3	0.52	−7.9	*Vcc7*	−0.12	−6
Lhr4	0.59	−6.4	*Vcc8*	0.45	−6.6
Lhr5	0.49	−6.5	*Vcc9*	0.46	−6.6
Lhr6	0.89	−6.5	*Vcc10*	0.63	−7.3
Lhr7	0.71	−7.2	*Vcc11*	−0.5	−6.8
Lhr8	0.71	−6.6	*Vcc12*	−0.28	−6.8
Lhr9	0.42	−6.3	*Vcc13*	0.77	−6.6
Lhr10	1.01	−6.5	*Vcc14*	−0.75	−5.9
Lhr11	0.21	−6.5	*Vcc15*	−0.57	−6
Lhr12	0.96	−7.3	*Vcc16*	−1.47	−5.6
Lhr13	0.95	−7.3	*Vcc17*	−1.78	−8.1
Lhr14	0.1	−5.4	*Vcc18*	−1.66	−6.4
Lhr15	0.85	−6.3	*Vdc1*	−0.5	−4.2
Lhr16	0.38	−6.8	*Vdc2*	−0.46	−4.1
Lhr17	0.4	−6.8	*Vdc3*	−0.72	−3.9
Lhr18	0.36	−6.4	*Vdc4*	−0.98	−3.8
Lhr19	0.81	−7.1	*Vdc5*	−1.04	−3.7
Lhr20	−1.15	−6.2	*pVcc1*	−1.74	−5.4
pVc1	−0.46	−6.1	*pVcc2*	−2.4	−5
pVc2	−0.5	−6.1	*pVac1*	−0.09	−10.1
pVc3	−0.79	−5.9	*pVac2*	0.38	−10.2

means that the isotopic composition of the fluid is controlled by the exchange with the rock mass. In such rock-buffered system the calcium carbonate, filling the fractures, largely originates from pressure dissolution of the rock matrix (Hudson, 1975; Ramsay, 1980). The numerous stylolites observed in the limestones, oriented parallel to the bedding could have provided the required calcium carbonate. However, an external fluid precipitating calcite cements with a similar stable isotopic composition as the limestone host-rock cannot be excluded. However, large-scale pre-Variscan cracks, providing secondary porosity along which extended fluid migration could have occurred, are absent.

6.2. Variscan vein cements

The stable isotopic composition of the Variscan calcite veins ranges between −8.1‰ and −5.6‰ VPDB for oxygen and between −1.78‰ and 0.86‰ VPDB for carbon (Fig. 7; Table 1). Values fall mainly within the range of the isotopic composition of the surrounding, non-dolomitised limestone. Three $\delta^{13}C$ values are lower than that of the host-rock. The $\delta^{18}O$ and the $\delta^{13}C$ values of the completely dolomitised limestones range, respectively, between −3.9‰ and −3.8‰ VPDB and between −0.78‰ and −0.60‰ VPDB (Fig. 8; Table 1). The stable isotopic composition of the Variscan dolomite veins ($\delta^{18}O = -4.2‰$ to −3.7‰ VPDB; $\delta^{13}C = -1.04‰$ to −0.46‰ VPDB) is similar to that of the surrounding dolomites (Fig. 8; Table 1).

Since dolomite veins are restricted to a dolostone host-rock and since the stable isotopic compositions of this host-rock and the veins are similar, precipitation of the dolomite veins occurred from a fluid whose composition was buffered by the rock (Gray et al., 1991; Marquer and Burkhard, 1992). The oxygen and

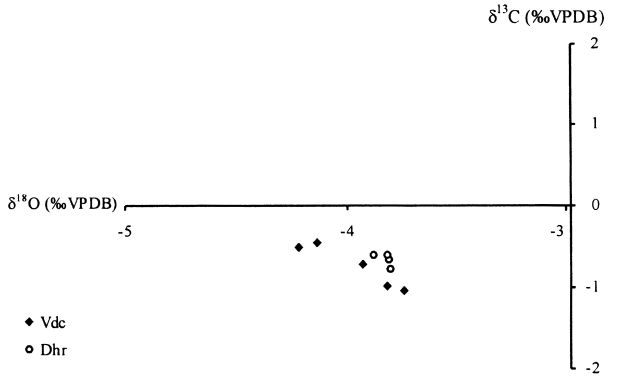

Fig. 8. Carbon and oxygen isotopic composition of the Variscan dolomite cements (Vdc, $n = 5$) and of the dolomitic host-rock (Dhr, $n = 4$).

carbon isotopic values of the calcite veins fall within the range of the limestones. Moreover, a comparison of the stable isotopic composition of the calcite and dolomite veins with that of the immediately surrounding limestones (at a distance ranging between 0.1 and 1 m) indicates $\delta^{18}O$ values and $\delta^{13}C$ values which may be similar or differ up to 1‰ (Fig. 9). These similarities in the isotopic data of calcite veins and limestone host-rock and the rock-buffered system present during formation of the dolomite veins are thought to be sufficiently indicative for a closed migration system during the precipitation of the calcite veins. The source of the calcium and bicarbonate for the precipitation of the veins is found in the numerous stylolites perpendicular to the bedding (layer-parallel-shortening stylolites). The lower $\delta^{13}C$ values of some of the veins compared to that of the immediately surrounding limestones can easily be explained by the maturation of the organic matter in these Givetian strata and the related release of ^{12}C during diagenesis (Irwin et al., 1977). The released ^{12}C of the organic matter has been incorporated in the calcite cements resulting in a lower $\delta^{13}C$ value than the limestone host-rock. The carbon of the organic matter present in the host rock is not incorporated in the analyses of the limestones. The same process could explain the three $\delta^{13}C$ values of the Variscan calcite cements lying outside the stable isotopic field of the host-rock. A closed fluid flow system is common at the Variscan front zone (Stroink, 1993; Hein and Behr, 1994). Only in the immediate vicinity of a set of imbricated thrust faults, has an open fluid flow system been proposed at this front zone (Muchez et al., 1998). Variscan calcite veins in an anticline just north of the major Midi thrust fault also formed in a rock-buffered system (Muchez et al., 1995).

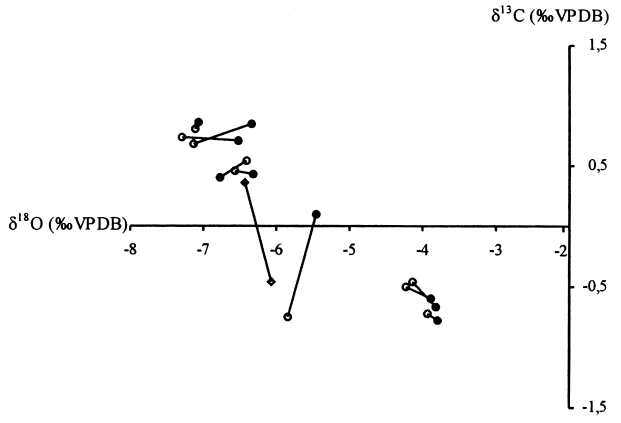

Fig. 9. Comparison of the stable isotope composition of the Pre-Variscan (black squares, $n = 1$) and Variscan (black dots, $n = 8$) vein cements with that of the immediately surrounding limestones (white dots and squares).

6.3. Post-Variscan vein cements

Only the carbonate veins of the post-Variscan fault V have been examined for their stable isotopic composition. The $\delta^{18}O$ and $\delta^{13}C$ values of the two iron-poor calcite samples are, respectively, −5.4‰ and −5.0‰ VPDB and −2.40‰ and −1.74‰ VPDB (Fig. 7; Table 1). The oxygen isotope values are close to those of the limestones. The more negative $\delta^{13}C$ values of the non-ferroan calcites compared with the host-rock can be explained by an additional contribution of ^{12}C with an organic origin (Irwin et al., 1977). The stable isotopic composition of the two ankerite samples are −10.2‰ and −10.1‰ VPDB for oxygen and −0.09‰ and 0.38‰ VPDB for carbon (Fig. 7; Table 1). These values show a significant difference with regard to the range of the surrounding Givetian limestones, especially taking into account $\Delta_{ankerite-calcite}$ of +3.2‰ (Longstaffe and Ayalon, 1987).

The trapping temperature of the iron-poor calcite sample corresponds to ~75°C (see Section 7.4). At this temperature, a calcite phase with an oxygen isotopic signature of ~−5.2‰ VPDB would have precipitated from a fluid with $\delta^{18}O$ of 4.8‰ SMOW (standard mean ocean water). Such a relatively high $\delta^{18}O$ value could be due to an important interaction of the fluid with the limestone host-rock. The different stable isotopic composition of the ankerite vein from that of the rock implies that after precipitation of the non-ferroan calcite phase the relatively closed system evolved towards an open one.

7. Fluid inclusion data

The fluid inclusions of four different groups (I, III, IV and V) were analysed to correlate the temperature–pressure conditions of vein cement precipitation with the related deformation events in the progressive folding of the Givetian limestones. Unfortunately, no suitable fluid inclusions for a microthermometric investigation have been found in group II. From all four groups, fluid inclusions occurring in growth zones were examined. Only these fluid inclusions are certain to have a primary origin and are suitable for deduction of the precipitation temperature and depth of the vein cements (Goldstein and Reynolds, 1994). The vein cements studied are interpreted to have formed in a rock-buffered system. In such a system the fluids are in mineralogical, geochemical and thermal equilibrium with the host rocks. A palaeogeothermal gradient of 50°C/km, determined by Muchez et al. (1991a) and Helsen (1995), has been applied to calculate the precipitation temperatures and depth from the isochores of the fluid inclusions. Although 50°C/km may seem to be high, it has been indicated by vitrinite reflectance

data, the conodont alteration indices and geothermal modelling (e.g. Lünenschloss et al., 1997; Lünenschloss, 1998). Although a lower palaeogeothermal gradient would result in higher precipitation temperatures and depths of the veins, it would not change the conclusions.

Re-equilibration of fluid inclusions to lower densities, inducing higher homogenisation temperatures, may occur during intracrystalline deformation of crystals. Microthermometric measurements were made in the vicinity of weakly strained zones of crystals (if present), while strongly deformed zones (e.g. twinned zones in calcite) were avoided to minimise the analyses of re-equilibrated inclusions. All fluid inclusions examined are two phases (liquid and gas) and located in growth zones. The fluid inclusions from the four groups in which the temperature of first melting (T_e) could be observed, have T_e values at or above −21°C. This indicates a dominantly H_2O–NaCl composition of the fluid inclusions in the veins analysed. The exact melting temperatures could not always be observed due to the small size of most fluid inclusions.

7.1. Group I: pre-Variscan deformation

The fluid inclusions are too small (2–3 μm) to allow determination of the melting temperatures (T_m). The homogenisation temperature (T_h) ranges between 221 and 286°C (Fig. 10). The measurements are made in crystals where an undulatory extinction and the occurrence of calcite twins indicate crystal-plastic deformation. Fluid inclusions were present within twin planes as well as in untwinned zones of the crystals.

Microthermometric data show a large range (65°C) of T_h values, which may be due to the intensive deformation of the calcite crystals. During deformation numerous re-equilibration phenomena affect the fluid inclusions and induce an increase in homogenisation temperature (Shepherd et al., 1985; Goldstein and Reynolds, 1994). However, fluid inclusions, which have not suffered the re-equilibration processes, could still be preserved. Minimum T_h values may represent those inclusions that preserved the fluid density during trapping (Muchez et al., 1991b). In a first instance a T_{hmin} of 221°C has been used to obtain an idea of the maximum initial trapping conditions of the pre-Variscan group. To know the trapping temperature (T_t) of the inclusions, a pressure correction should be applied to the T_h values. The trapping temperatures and pressures are deduced from the intersection of the isochores for the H_2O–NaCl inclusions and a palaeolithostatic gradient of 50°C/26 MPa (Muchez et al., 1991a; Helsen, 1995). The isochores for the H_2O–NaCl inclusions have been calculated using the program FLINCOR (Brown, 1989) and the equations of Brown and Lamb (1989) for the H_2O–NaCl system applied to the hom-

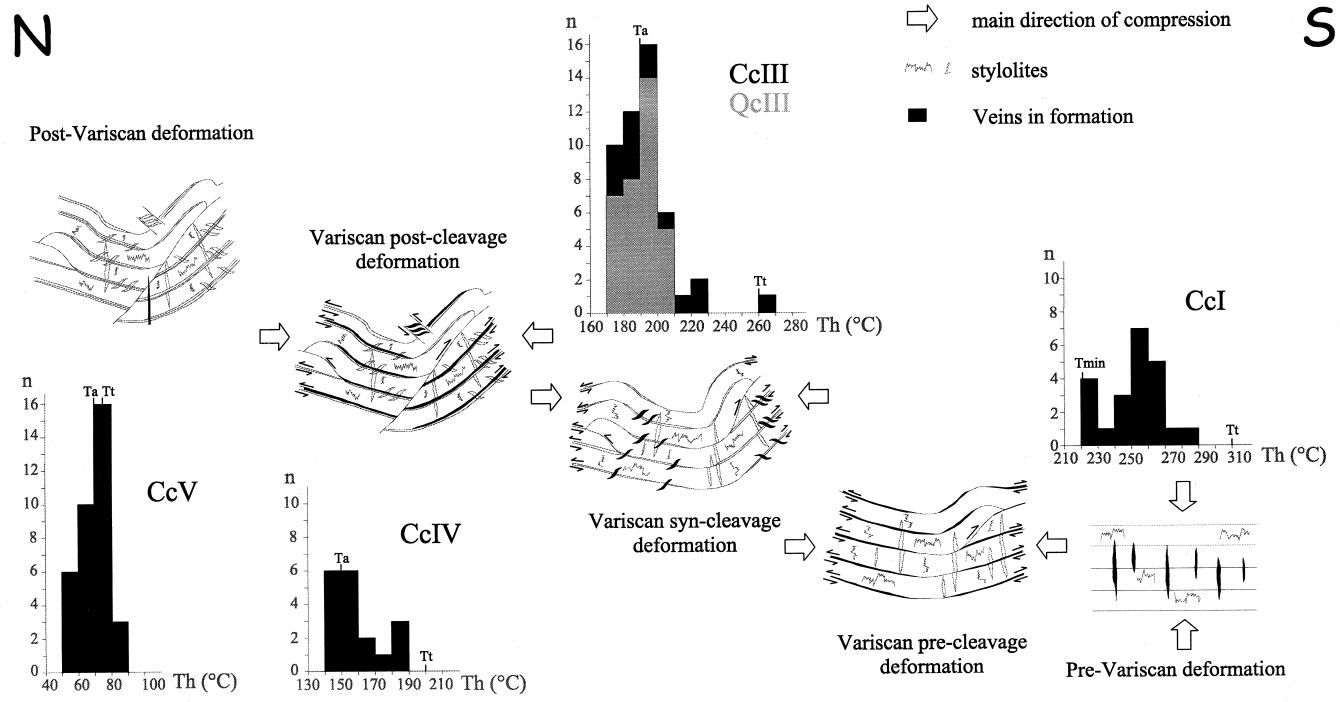

Fig. 10. Primary fluid inclusion data of the different vein groups, expressing the protracted deformation history of the syncline. At each stage, active veining is indicated in bold. CcI — pre-Variscan group I calcites. CcIII — Variscan group III calcite. QcIII — Variscan group III quartz. CcIV — Variscan group IV calcites. CcV — post-Variscan group V calcites. n — number of analyses. T_h — homogenisation temperatures. T_a — average homogenisation temperature. T_t — trapping temperature.

ogenisation temperature of 221°C and an average salinity of 12.3 eq.wt% NaCl of the group III Variscan fluids (see below). The latter is thought to be justified because of the proposed closed fluid system present before and during the Variscan deformation. The calculated T_t value for the pre-Variscan group is 310°C. This temperature corresponds to a pressure of 150 MPa and a precipitation depth of 5700 m. However since the calcites are strongly deformed, lower homogenisation temperatures could have been present originally. Therefore 5700 m is regarded as a maximum depth.

7.2. Group III: Variscan deformation, syn-cleavage

The homogenisation temperature of the primary fluid inclusions (3–6 μm) in group III calcite crystals ranges between 173 and 265°C (Fig. 10). The petrographic study shows that homogenisation temperatures between 173 and 203°C are restricted to calcite crystals with a weak development of twin planes. Temperatures above 203°C are restricted to the fluid inclusions in the volumetrically more important, intensely twinned crystals. The inclusions of the intensely twinned crystals have probably been stretched (see also Goldstein and Reynolds, 1994) and are therefore not representative of the original homogenisation temperature. Homogenisation temperatures of measurements of the fluid inclusions (3–10 μm) in group III quartz crystals ranges between 171 and 206°C with an average of 190°C (Fig. 10). The only optical feature observed in the quartz crystals, which is associated with intracrystalline deformation by dislocation creep, is sweeping undulatory extinction. Dynamic recrystallisation of the crystals, which could induce a marked increase of filling temperatures, has not been observed. Taking into account the higher resistance of quartz crystals to deformation (Shepherd et al., 1985; Goldstein and Reynolds, 1994) and the similarity between the T_h values of the fluid inclusions of the quartz and weakly deformed calcite crystals, 171–206°C can be assumed to be the T_h range of the fluid inclusions which have preserved the original fluid density. It further supports the assumption that all fluid inclusions above 206°C have been re-equilibrated, inducing higher homogenisation temperatures.

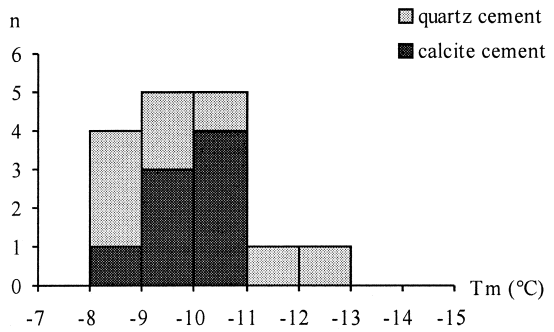

Fig. 11. Melting temperatures T_m of the Variscan group III calcite and quartz cement (n = 16).

The final melting temperatures of the group III calcite and quartz crystals all lie between −8.0 and −12.8°C (Fig. 11), corresponding to a salinity of 12–16 eq.wt% NaCl. This salinity is much higher than the salinity of the seawater in which the Givetian limestones have been deposited. At first sight, this could be regarded as an argument for an external source of the fluids migrating through the Givetian during the Variscan deformation in contradiction with the former interpretation. However, high salinity fluids formed in evaporitic basins (e.g. Tournai area) during and after the Givetian (Dejonghe et al., 1998). These fluids could have migrated laterally and downwards into the more open marine limestones due to their high density and this during early diagenesis. The migration of the dense high salinity fluids could have caused the dolomitisation of the Givetian limestones. Similar processes have been identified in eastern Belgium where reflux dolomitisation of open marine limestones occurred (Nielsen et al., 1994) and was responsible for the origin of high salinity H_2O–NaCl–$CaCl_2$ fluids in the deeper subsurface (Heijlen et al., 1999).

A pressure correction was applied to the average T_h value of 190°C in the same way as described above. The average trapping temperature is 260°C and corresponds to a trapping pressure of 120 MPa. This means that the veins could have formed at a depth of ~4700 m.

7.3. Group IV: Variscan deformation: post-cleavage

The fluid inclusions of the calcites of the fourth group (second subgroup) are very small (2–4 μm). Homogenisation temperatures range between 140 and 190°C (Fig. 10). A petrographic study shows that homogenisation temperatures above 165°C are restricted to fluid inclusions associated with twin planes whereas temperatures between 140 and 158°C with an average of 150°C are measured in zones mainly without twins. The fluid inclusions in the twinned parts have probably been stretched (see Goldstein and Reynolds, 1994). Therefore only the lower temperature range (140–158°C) is considered representative for the original homogenisation temperature. After application of a pressure correction to the average T_h value of 150°C, a trapping temperature of 200°C is obtained. Taking into account a surface temperature of 25°C and a lithostatic gradient of 50°C/26 MPa, 200°C corresponds to a trapping pressure of 90 MPa and a precipitation depth of ~3500 m.

7.4. Group V: Post-Variscan deformation

The fluid inclusions studied in the non-ferroan calcites of this group are very small (2–3 μm). Homogenisation temperatures range between 51 and 86°C with an average of 70°C (Fig. 10). Because of the low T_h values and the presence of large open fractures at the time of precipitation, a hydrostatic pressure correction of 50°C/10 MPa was applied to obtain an average trapping temperature of 75°C. This corresponds to a trapping pressure of ~10 MPa and a formation depth of ~1000 m.

8. Discussion

A formation temperature of 310°C has been calculated for the pre-Variscan veins, which corresponds to a precipitation depth of 5700 m. However, because of the long time period involved in the Variscan deformation, the possibility that all fluid inclusions have been re-equilibrated must be considered. This would imply that 5700 m is a maximum value and that the exact formation depth of the veins cannot be obtained. A limit can be set to the minimum depth of burial by the microthermometric results of the quartz crystals of the sigmoidal veins of group III. Because of a much higher resistance to deformation of quartz crystals (Shepherd et al., 1985; Goldstein and Reynolds, 1994), the homogenisation temperatures of this generation (171–206°C) may represent reliable values. These values yield a minimum for the burial depth of 4700 m. Colour alteration index (CAI) values of conodonts of the Givetian limestones in the area of Bettrechies correspond to 4.5–5.0, which implies a palaeotemperature of 245–310°C (Helsen, 1995). The vitrinite reflectance of a limited number of particles lies between 3.5 and 4 (Degardin, personal communication, 1998). According to Barker and Goldstein (1990), vitrinite reflectance values of 3.5–4 reflect temperatures between 310 and 330°C. The agreement between the calculated trapping temperature of the fluid inclusions and the CAI and vitrinite data indicate that a maximum burial temperature of 310°C for the Givetian strata cannot be excluded.

In the microthermometric study a constant geothermal gradient of 50°C/26 MPa has been used to calculate the trapping conditions of the fluid inclusions in order to obtain a relative deformation-depth history of the frontal zone of the Ardenne Allochthon. A chronologically decreasing precipitation temperature has been suggested, reflecting a decreasing depth evolution during progressive folding.

However, the possibility that the decreasing homogenisation temperatures do not actually indicate a decreasing depth evolution but are the reflection of a decreasing geothermal gradient should be considered. This would imply that all vein generations may have formed at the same depth and were passively transported upwards during transport along the Midi fault. This implies a model where the final overthrusting along the Variscan thrust front must therefore postdate the major part of the Variscan deformation and is in accordance with Fourmarier's model considering a cleavage as a burial phenomenon which needs at least an overburden of 5–6 km (Fourmarier, 1939). If a constant depth of 5700 m is assumed for the folding of the syncline and vein formation, then the geothermal gradient decreased from 50 to 30°C during the Variscan. Schroyen and Muchez (2000) examined fluid inclusions in six successive quartz generations at the southern border of the Stavelot–Venn Massif (Belgium) (Fig. 1). These six quartz generations formed during the Variscan deformation and are mainly related to large thrust faults. If thrusting post-dates the main Variscan deformation, a geothermal gradient of 30°C would have been present during this thrusting. P–T formation conditions were calculated using H_2O–CO_2–NaCl, fluid inclusion isochores, total homogenisation temperatures and geothermometry results of syngenetic chlorite minerals. All Variscan quartz generations indicate a geothermal gradient between 40 and 50°C. Considering the fact that the Variscan veins show an identical geothermal gradient and that independent studies all point towards a geothermal gradient of ~50°C (Muchez et al., 1991a; Helsen, 1995), we think that the assumption of a constant geothermal gradient of 50°C/km is more likely than considering a drop in geothermal gradient. Therefore in our model, the decreasing evolution in formation temperature of the veins is interpreted to indicate that the syncline did not develop at a specific depth, but rather as an active, progressive deformation process during transport along the Variscan thrust front.

9. Conclusions

In the syncline at Bettrechies different vein generations can be observed that formed before, during and after the Variscan deformation. Structural and petrographic data have been used to distinguish five major groups of veins (pre-Variscan, Variscan pre-cleavage, Variscan syn-cleavage, Variscan post-cleavage and post-Variscan deformation). Each group can be correlated with a specific structural episode in the development of the syncline. Mineral and stable isotope analysis has been applied to characterise the nature of the fluid system (closed rather than other) in the Givetian limestones. The pre- and syn-Variscan vein cements, and one post-Variscan calcite phase, show similar mineralogies and oxygen and carbon isotopic

compositions to the surrounding host-rock. They are interpreted to have been precipitated from a fluid whose composition was largely buffered by the host limestones. The numerous stylolites present in the quarry provide further support for this interpretation. The stable isotopic composition of a post-Variscan ankerite phase indicates an evolution of the closed fluid flow system towards an open one during the post-Variscan stage.

The microthermometric study of primary fluid inclusions constrains the P–T conditions of vein precipitation and possibly the front zone of the Ardenne Allochthon. During burial of the Givetian limestones, veins oriented perpendicular to the bedding formed at a depth of $\leq$5700 m. During the Variscan deformation, the limestones were folded and thrust along the south-dipping Midi fault. At a first stage within this period, veins parallel to the bedding and two other generations related to the movement of ramp faults were formed. At a second stage (syn-cleavage), sigmoidal veins precipitated. Fluid inclusion data indicate a precipitation depth of ~4700 m. During a third stage of the Variscan deformation veins parallel to the bedding formed at a depth of ~3500 m. The difference in trapping temperature of the primary fluid inclusions and possibly of the formation depth of the Variscan veins, is interpreted to indicate that the protracted development of the syncline took place at decreasing depth/temperatures during transport along the Variscan front thrust.

Acknowledgements

We would like to thank K. O'Hara and M. Burkhard for their helpful and constructive reviews and R.J. Lisle for correcting the manuscript. We also thank H. Nijs for the careful preparation of the doubly polished sections. Ph. Muchez and M. Sintubin are, respectively, senior research associate and postdoctoral fellow of the Fund of Scientific Research of Flanders, Belgium. The SECAB company is thanked for its cooperation during the fieldwork. We are grateful to E. Keppens of the Vrije Universiteit Brussel for the isotopic analysis.

References

Barker, C.E., Goldstein, R.H., 1990. Fluid-inclusion technique for determining maximum temperature in calcite and its comparison to the vitrinite reflectance geothermometer. Geology 18, 1003–1006.

Boulvain, F., Coen-Aubert, M., Mansy, J.-L., Proust, J.N., 1994. Glageon: une coupe de Givétien en Avesnois (France). Sédimentologie, coraux, géologie régionale, diagenèse. Bulletin de la Société belge de Geologie 103, 171–203.

Brown, P.E., 1989. Flincor: A microcomputer program for the reduction and investigation of fluid inclusion data. American Mineralogist 74, 1390–1393.

Brown, P.E., Lamb, W.M., 1989. P–V–T properties of fluids in the system H_2O–CO_2–NaCl: new graphical presentations and implications for fluid inclusion studies. Geochimica et Cosmochimica Acta 53, 1209–1221.

Bultynck, P., Coen-Aubert, M., Dejonghe, L., Godefroid, J., Hance, L., Lacroix, D., Préat, A., Stainier, P., Steemans, Ph., Streel, M., Tourneur, F., 1991. Les formations du Dévonien moyen de la Belgique. Mémoires pour servir à l'explication des Cartes géologiques et minières de la Belgique 30.

Burkhard, M., Kerrich, R., 1988. Fluid regimes in the deformation of the Helvetic nappes, Switzerland, as inferred from stable isotope data. Contributions to Mineralogy and Petrology 99, 416–429.

Burkhard, M., 1993. Calcite twins, their geometry appearance and significance as stress–strain markers and indicators of tectonic regime: a review. Journal of Structural Geology 15, 351–368.

Craig, H., 1957. Isotopic standards for carbon and oxygen correction factors for mass spectrometric analysis for carbon dioxide. Geochimica et Cosmochimica Acta 12, 133–149.

Dejonghe, L., Demaiffe, D., Weis, D., 1998. Strontium isotope geochemistry of anhydrite and calcite pseudomorphs after anhydrite from Palaeozoic formations in Belgium. Chemical Geology 144, 63–71.

Dickson, J.A.D., 1966. Carbonate identification and genesis as revealed by staining. Journal of Sedimentary Petrology 36, 491–505.

Fischer, D., Byrne, T., 1990. The character and distribution of mineralized fractures in the Kodiak Formation, Alaska: implications for fluid flow in an underthrust sequence. Journal of Geophysical Research 95, 9069–9080.

Fourmarier, P., 1939. Quelques résultats de l'étude de schistosité dans la bande silurienne de Sambre-et-Meuse. Annales de la Société Géologique de Belgique 63, B16–B24.

Goldstein, R., Reynolds, J., 1994. Systematics of fluid inclusions in diagenetic minerals. Society for Sedimentary Geology. Short Course 31.

Gray, D.R., Gregory, R.T., Durney, D.W., 1991. Rock-buffered fluid–rock interaction in deformed quartz-rich turbidite sequences, Eastern Australia. Journal of Geophysical Research 96, 19681–19704.

Heijlen, W., Muchez, P., Van Hoof, P., Banks, D. 1999. Origin of Pb–Zn mineralising fluids in the Variscides of Belgium. In: Stanley, et al. (Eds.), Mineral Deposits: Processes to Processing. Belkema, Rotterdam, pp. 869–872.

Hein, U.F., Behr, H.J., 1994. Lagerstättenbildung durch Tectonic Brines — Überprüfung eines Modells am Beispiel synorogener variskischer Vererzungen Mitteleuropas. Beihefte zum European Journal of Mineralogy 6.

Helsen, S., 1995. Burial history of Palaeozoic strata in Belgium and adjacent areas based on conodont alteration data. PhD. thesis, Katholieke Universiteit Leuven.

Hodgkins, M.A., Stewart, K.G., 1994. The use of fluid inclusions to constrain fault zone pressure, temperature and kinematic history: an example from the Alpi Apuane, Italy. Journal of Structural Geology 16, 85–96.

Hudson, J.D., 1975. Carbon isotopes and limestone cement. Geology 3, 18–22.

Irwin, H., Curtis, C., Coleman, M., 1977. Isotopic evidence for source of diagenetic carbonates formed during burial of organic-rich sediments. Nature 269, 209–213.

Khatir, A., 1990. Structuration et déformation progressive au front de l'allochtone ardennais (Nord de la France). Annales de la Société géologique du Nord 18.

Kirschner, D.L., Sharp, Z.D., Masson, H., 1995. Oxygen isotope

thermometry of quartz–calcite veins: Unraveling the thermal-tectonic history of the subgreenschist facies Morcles nappe (Swiss Alps). Geological Society of America Bulletin 107, 1145–1156.

Lacquement, F., 1996. Les mécanismes du plissement au niveau d'un front de déformation: exemple du front Varisque Ardennais. Mémoire DEA, Université des Sciences et Technologie de Lille.

Longstaffe, F.J., Ayalon, A., 1987. Oxygen-isotope studies of clastic diagenesis in the Lower Cretaceous Viking Formation, Alberta: implications for the role of meteoric water. In: Marshall, J.D. (Ed.), Diagenesis of Sedimentary Sequences, Geological Society Special Publication, 36, pp. 277–296.

Lünenschloss, B., Bayer, U., Muchez, Ph., 1997. Coalification anomalies induced by fluid flow at the Variscan thrust front: A numerical model of the palaeotemperature field. Geologie en Mijnbouw 76, 271–275.

Lünenschloss, B., 1998. Modellierung der Temperatur- und Fluidgeschichte an der variszichen Front (Verviers-Synklinorium und Nordeifel). Scientific Technical Report STR98/07, Geoforschungszentrum Potsdam, Germany.

Mansy, J.-L., Meilliez, F., Mercier, E., Khatir, A., Boulvain, F., 1995. Le rôle du plissement disharmonique dans la tectonogenèse de l'allochtone ardennais. Bulletin de la Société géologique de France 166, 295–302.

Mansy, J.-L., Lacquement, F., Meilliez, F., Hanot, F., Everaerts, M., 1997. Interprétation d'un profil sismique pétrolier, sur le méridien de Valenciennes (Nord de la France). Aardkundige Mededelingen 8, 127–129.

Marquer, D., Burkhard, M., 1992. Fluid circulation, progressive deformation and mass-transfer processes in the upper crust: the example of basement–cover relationship in the External Crystalline Massifs, Switzerland. Journal of Structural Geology 14, 1047–1057.

Meere, P.A., Banks, D.A., 1997. Upper crustal fluid migration: an example from the Variscides of SW Ireland. Journal of the Geological Society of London 154, 975–985.

Meyers, W.J., Lohmann, K.C., 1985. Isotope geochemistry of regionally extensive calcite cement zones and marine components in Mississippian limestones, New Mexico. In: Sneidermann, N., Harris, P.M. (Eds.), Carbonate Cements, Society of Economic Paleontologists and Mineralogists, Special Publication, 36, pp. 223–239.

Moore, J.C., Mascle, A., Taylor, E., Andreieff, P., Alvarez, F., Barnes, R., Beck, C., Behrmann, J., Blanc, G., Brown, K., Clark, M., Dolan, J., Fisher, A., Gieskes, J., Hounslow, M., McLellan, P., Moran, K., Ogawa, Y., Sakai, T., Schoonmaker, J., Vrolijk, P., Wilkens, R., Williams, C., 1988. Tectonics and hydrogeology of the northern Barbados Ridge: Results from Ocean Drilling Program Leg 110. Geological Society of America Bulletin 100, 1578–1593.

Moore, J.C., Orange, D., Kulm, L.D., 1990. Interrelationship of fluid venting and structural evolution: Alvin observations from the Frontal Accretionary Prism, Oregon. Journal of Geophysical Research 98, 8795–8808.

Muchez, P., Boven, J., Bouckaert, J., Leplat, P., Viaene, W., Wolf, M., 1991a. Illite crystallinity in the Carboniferous of the Campine–Brabant Basin (Belgium) and its relationship to organic maturity indicators. Neues Jahrbuch für Geologie und Paläontologie Abhandlungen 182, 117–131.

Muchez, P., Viaene, W.A., Keppens, E., Marshall, J.D., Vandenberghe, N., 1991b. Vein cements and the geochemical evolution of subsurface fluids in the Visean of the Campine Basin (Poederlee borehole, Belgium). Journal of the Geological Society of London 148, 1005–1117.

Muchez, P., Marshall, J.D., Touret, J.L.R., Viaene, W.A., 1994. Origin and migration of palaeofluids in the Upper Visean of the Campine Basin, northern Belgium. Sedimentology 41, 133–145.

Muchez, Ph., Slobodnik, M., Viaene, W., Keppens, E., 1995. Geochemical constraints on the origin and migration of palaeofluids at the northern margin of the Variscan foreland, southern Belgium. Sedimentary Geology 96, 191–200.

Nielsen, P., Swennen, R., Keppens, E., 1994. Multiple-step recrystallization within massive ancient dolomite units: an example from the Dinantian of Belgium. Sedimentology 41, 567–584.

O'Hara, K., Haak, A., 1992. A fluid inclusion study of fluid pressure and salinity variations in the footwall of the Rector Branch thrust, North Carolina, USA. Journal of Structural Geology 14, 579–589.

Ramsay, J.G., 1980. The crack–seal mechanism of rock deformation. Nature 284, 135–139.

Ramsay, J.G., Huber, M.I., 1983. The Techniques of Modern Structural Geology, vol. 1: Strain analysis. Academic Press, London.

Schroyen, K., Muchez, P., 2000. Evolution of metamorphic fluids at the Variscan-fold-and-thrust belt in eastern Belgium. Sedimentary Geology, in press.

Shepherd, T., Rankin, A.H., Alderton, D.H.M., 1985. A Practical Guide to Fluid Inclusion Studies. Blackie, London.

Stroink, L., 1993. Zur Diagenese paläozoischer Sandsteine am Nordrand des Linksrheinisch-Ardennischen Schiefergebirges. Aachener Geowissenschaftliche Beiträge 1.

Tobin, H.J., Moore, J.C., MacKay, M.E., Orange, D.L., Kulm, L.D., 1993. Fluid flow along a strike-slip fault at the toe of the Oregon accretionary prism: implications for the geometry of frontal accretion. Geological Society of America Bulletin 105, 569–582.

Vrolijk, P., 1987. Tectonically driven fluid flow in the Kodiak accretionary complex, Alaska. Geology 15, 466–469.